PCCP

Accepted Manuscript

ROYAL SOCIETY OF CHEMISTRY

www.rsc.org/pccp

Reactive molecular simulations of protonation of water clusters and depletion of acidity in H-ZSM-5 zeolite

Kaushik L. Joshi, George Psofogiannakis and Adri C.T. van Duin*

Department of Mechanical and Nuclear Engineering
Pennsylvania State University, University Park, PA 16801

Sumathy Raman
ExxonMobil Research and Engineering, Annandale, NJ, 08801

Abstract

Using reactive molecular dynamics (RMD), we present an atomistic insight into the interaction between water molecules and acidic centers of H-ZSM-5 zeolite. The reactive force field method, ReaxFF was used to evaluate the adsorption and diffusion of water as well as to study the protonation of water molecules inside zeolite channels. The existing Si/Al/O/H parameters were refitted against DFT calculations to improve the ReaxFF description of interaction between water molecules and the acidic sites of zeolites. The diffusion coefficient of water in the zeolite obtained from refitted parameters is in excellent agreement with experimental results. The molecular dynamics (MD) simulations indicate that protonation of water molecules and acidity of the zeolite catalyst depends on water loadings and temperature and the observed trends compare favorably with existing experimental and theoretical studies. At higher water loadings, protonation of water molecules is more frequent leading to formation and growth of protonated water clusters inside zeolite channels. From the analysis of various reaction channels that were observed during the simulations, we found that such water clusters have relatively short life due to frequent interchange of protons and water molecules among the water clusters. Such proton hopping events play a key role in moving the protons between different acidic centers of zeolite. These simulations show the capability of ReaxFF in providing atomistic details of complex chemical interactions between water phase and solid acid zeolites.

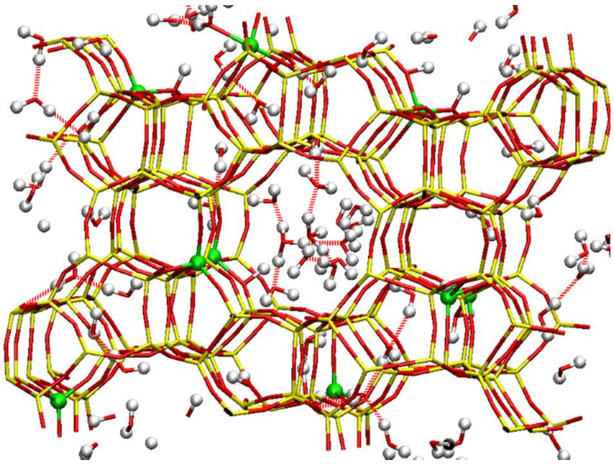

Introduction

Zeolites are microporous materials that are widely used as solid catalysts in petroleum and chemical industries because of their adsorption capacity, shape selectivity and flexible acidity [1]. Zeolites are classified into different types based on their composition, pore size and channel systems. Silicalite is an-all silica MFI zeolite consisting of tetrahedral framework of SiO_4 connected through shared oxygen atoms. ZSM-5 zeolites are synthesized by substituting few silicon atoms (Si^{4+}) by aluminum (Al^{3+}) atoms [2]. Protons (H^+) are exchanged on the neighboring oxygen atoms in H-ZSM-5 to maintain the charge neutrality. The location and population of such hydroxyl groups determine the acidity of the overall framework. The [Si-O-(Si-O) $_n$-Si] sequences in the framework are hydrophobic, while the bridging Si-OH-Al groups of the framework are strongly acidic [3]. Although it is widely accepted that water molecules are strongly adsorbed at these acidic centers leading to formation of protonated water clusters at higher water loadings, the atomistic knowledge of such interactions between water molecules and acidic centers is still incomplete.

The interaction of water molecules with H-zeolites has been studied both experimentally and computationally. Wakabayashi, Kondo, Domen and Hirose[4] studied the adsorption of water inside the H-ZSM-5 zeolite by means of FTIR and found the IR spectroscopic evidence for H-bonded adsorption of water on acidic OH sites. In a similar FTIR investigation by Bordiga et al.[5], it was shown that at low water loadings, water molecules form hydrogen bonded-adducts with H-ZSM-5 zeolite while at high water loadings, these adducts are transformed into $H^+(H_2O)_n$ ionic species. A recent FTIR investigation indicated that the tendency to form protonated water clusters depends upon temperature and at elevated temperatures, such a transformation into ionic species occurs only to a limited extent[6]. Along with FTIR, neutron diffraction technique has also been used to study acidity of zeolites in the presence of water. Smith et al.[7] identified H_3O^+ ion using powder neutron diffraction on HSAPO-34 zeolite. Alberti and Martucci[8] found that acidic protons have remarkable mobility in low silica ferrierite. They attributed this mobility to various proton transfer mechanisms where water molecules or water clusters act as proton carriers.

Computationally, the interaction between water molecules and zeolite framework has been studied using both, electronic structure methods and molecular dynamics/Monte Carlo methods. In ab initio calculations, to reduce computational cost, the zeolite framework was often approximated by cluster models with Brønsted acidic sites[9,10,11]. In such calculations, it was shown that adsorption adduct is a minimum on the potential energy surface whereas the hydroxonium ion corresponds to a transition structure for the proton exchange and at least three water molecules must be involved to complete a proton transfer from zeolite to water[12]. However, larger models and description of dynamics effects are essential for studying adsorption and protonation at higher water loadings. An ab initio molecular dynamics study[13] on periodic model of HSAPO-34 found that the acidic site in HSAPO-34 can protonate water dimer, but not single isolated water molecule. Recently, Vener, Rozanska and Sauer performed Car-Parrinello molecular dynamics on periodic model of H-SSZ-13 for various water loadings[14]. They observed the following patterns.

- Single water molecules are not protonated
- Protonated water dimer is not stable
- Water tetramer can exist but only for short duration of time
- The protonated water tetramer is the smallest stable protonated water cluster at finite temperature.

Based on their calculations, the authors also concluded that, with increase in temperature, protons tend to move back to the zeolite framework.

Many MD and grand canonical Monte Carlo simulations(GCMC) have been done using various force field methods to study diffusivity and adsorption of water in different types of zeolites[15,16,17,18]. It was observed that, due to the hydrophobicity of silicalite pore system, water adsorption is minimal until critical pressure beyond which pores become saturated with water molecules[19]. Adsorption of water is significantly enhanced in the presence of defects such as silanol groups and extra-framework cations. It was also found that silanol defects have little effect on water diffusivity. However, the cation defects significantly change structure of water clusters inside the pores thereby reducing the self diffusivity of water inside silicalite pores[20].

Besides zeolite-water cluster interactions, ample information is available in the literature on protonated water clusters in condensed phase. Hydrated proton play important role in many biological and materials systems and hence has been subject of both experimental[21,22] and ab-initio calculations[23,24]. Reactive potentials have also been used to study proton transfer dynamics in MD simulations[25,26]. However, none of these atomistic simulations directly address protonation of water clusters inside porous acidic zeolite. In this work, our aim is to study the effects of temperature and water loadings on protonation of water inside H-ZSM-5 zeolite using the ReaxFF reactive force field method.

Simulation Methods

ReaxFF reactive force field method

ReaxFF is a reactive force field that can model bond breaking and bond formation on the fly during MD simulation[27]. This force field approach combines a bond order/bond distance relationship with a polarizable charge description and bond-order dependent many body (3 and 4-body) interactions. The combination of covalent and Coulomb interactions has made ReaxFF applicable to a wide range of materials, including covalent[28,29], metallic[30,31] and metal hydride/oxide/carbide[32,33] systems. A more detailed description of the force field can be found in Ref 21.

Force Field Refitting and validation

In this work we have used a modified version (see Supporting Info) of the previously tested Si/Al/O/H ReaxFF force field[34]. The previous version of the force field was parameterized against an extensive set of DFT data, including equations of state for several aluminosilicate phases, silicon and silicon oxide interfaces, silicon-water interactions and aluminum oxidation/hydrogenation energies, as well as bond stretching and angle bending energies. That force field was able to predict the hydrogen migration pathways in the absence of water sufficiently well. To predict more accurately the strength of interaction and potential energy surface between water molecules and the acidic protons of aluminosilicate models, a subset of the parameters were refitted against DFT calculations. Re-fitting of some parameters pertaining to the Al-O bond and the associated non-bonded interactions and angle terms, was kept minimal so as not to affect previous predictions of the aluminosilicate force-field to any significant extent. None of the parameters that are associated with the Si/O/H system or the water part of the force-field were changed.

Previous DFT calculations[35] for the H-ZSM5 zeolite have shown that the H migration (hopping) mechanism is assisted by the specific interaction of the acidic H with the water molecule, which stabilizes the transition state, allowing for a low-barrier migration pathway. The water-assisted migration pathway is shown in Fig. 1. The reaction coordinate scan was obtained using DFT[36] with B3LYP functional and 6-311G++** basis set for all elements. Fig. 2 shows the energy plotted against d-d(f), where d is the distance shown in the inset, representing the formation of O-H bond and d(f) is its value in the final state. It can be seen that proton migration, for this particular cluster model, is not a symmetric pathway as water molecule has a different binding energy in the two end states. The calculated DFT energy barrier for proton migration is 6.8 kcal/mol which is in excellent agreement with the previous calculations[35]. The reaction pathway from ReaxFF is qualitatively similar to the DFT pathway and the ReaxFF energy difference between final, transition and initial states is also in excellent agreement with DFT calculations.

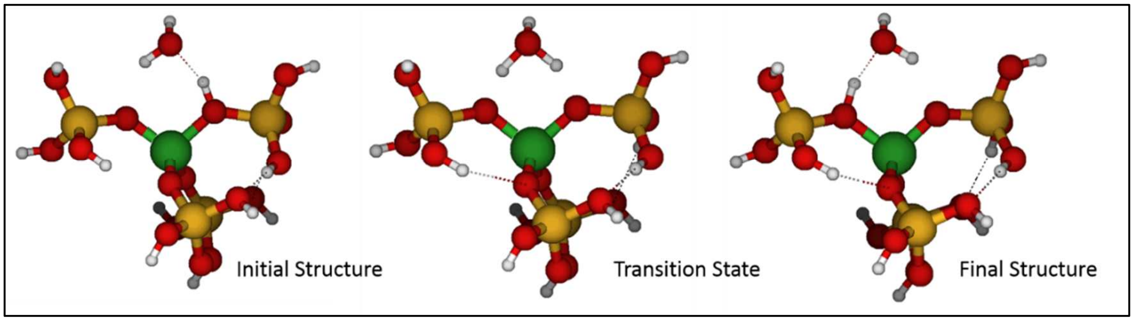

Fig 1 Water assisted proton migration from DFT calculations. The transition state is stabilized via interaction of the acidic H with a H_2O molecule. Al = Green, Si = Yellow, O = Red, H = White.

To further validate the force field for zeolite-water interactions, we compared ReaxFF predictions for the adsorption energy of water on acidic sites with existing DFT calculations for both the cluster and periodic models. For the cluster model shown in Figure 1, the refitted ReaxFF parameters predict the water adsorption energy to be 16.9 kcal/mol, which is in excellent agreement with previous DFT cluster calculations by Ryder et al.[30] (16.9 kcal/mol), whereas our own DFT methodology predicts a slightly higher interaction energy (20.2 kcal/mol). Like cluster models, the adsorption energy for periodic models depends upon the method/functionals used e.g. Chiu, Vayssilov, Genest, Borgna and Rösch[37] reported adsorption energy of 17.2 kcal /mol for vdW-DF2, 17.9 Kcal/mol for PBE and 22.2 Kcal/mol for PBE-D. We tested the ReaxFF for an extended zeolite model by computing the adsorption energy of a single water molecule inside 10 member ring of the H-ZSM-5 periodic model shown in Fig. 3. The ReaxFF prediction for the.

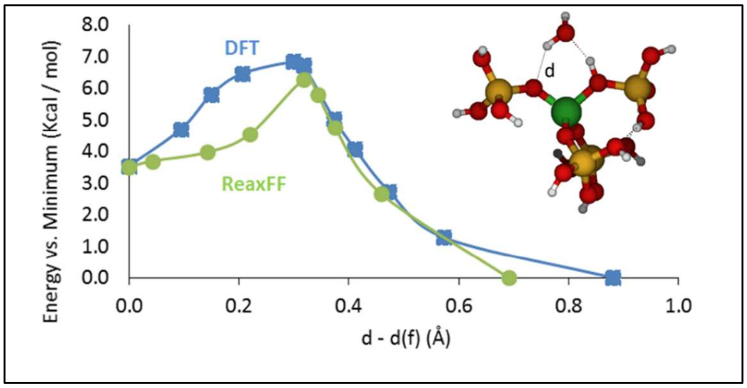

Fig. 2 Energy versus reaction coordinate for the water-assisted proton migration pathway, as predicted by DFT and ReaxFF. The inset shows the minimum-energy initial structure.

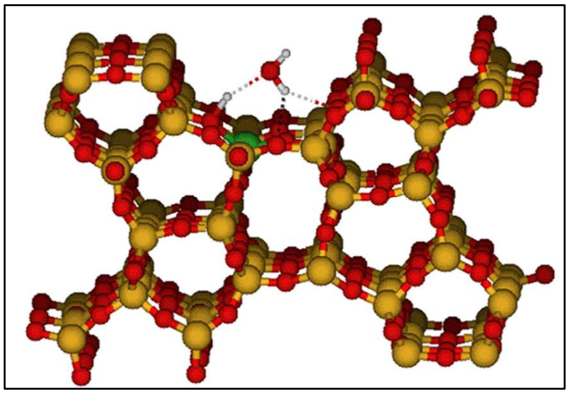

Fig. 3 Unit cell and ReaxFF optimized structure of a water molecule interacting with the proton in a 10-member ring of an orthogonal 289-atom periodic model of H-ZSM5.

adsorption energy is 15.4 kcal/mol. Based on the above calculations; we can conclude that the ReaxFF predictions are quite reasonable for adsorption of water inside acidic zeolite frameworks

MD Simulations

After refitting and validating the force field, we performed MD simulations to study diffusivity and reactivity of water inside zeolite pores. For evaluating the diffusion coefficient of water, we performed MD simulations inside silicalite and H-ZSM-5 zeolite. Silicalite model consisted of a periodic framework of 576 atoms (192 Si atoms, 384 O atoms). The H-ZSM-5 zeolite was constructed by substituting 9 T12 Si atoms with Al and then adding protons on the corresponding oxygen atoms. To mimic experimental conditions, 2 water molecules per Al atom were placed randomly inside the channels of the zeolite framework. The MD simulations were performed in NVT ensemble with Berendsen thermostat[38]. Each system was initially equilibrated for 500ps and then each simulation was performed for 1.5ns with a timestep of 0.25 fs to collect statistics. The diffusion coefficients were evaluated at 300K, 400K and 500K for silicalite and at 300K, 350K, 400K, 450K and 500K for H-ZSM-5 zeolite. The zeolite framework atoms were free to move during the simulation. The self diffusion coefficient is calculated using Einstein's equation

$$D = \frac{1}{6}\lim_{t\to\infty}\frac{d}{dt}\langle|r(t) - r(0)|^2\rangle \qquad (1)$$

To improve statistics, the calculation of the ensemble-averaged mean squared displacement in equation 1 was implemented using the standard blocks averaging and shifting register techniques[39]. Mean-squared displacements along each direction were calculated from a series of time origins t_i. The ensemble average was computed using equation 2.

$$\langle|r(t) - r(0)|^2\rangle = \frac{1}{N_{atoms}\, N_{origin}}\sum_{i=1}^{N_{origin}}\sum_{j=1}^{N_{atoms}}(r_j(t_i + t) - r_j(t))^2 \qquad (2)$$

where N_{origin} is the number of time origins t_i used in each block.

For studying the reactivity of water molecules, the H-ZSM-5 zeolite containing 9 Al atoms was used as a solid acid. The simulations were done with one, two, three, four, eight and ten water molecules per acidic site. For every H_2O-Al ratio, NVT simulations were performed at 350K, 400K and 500K. The MD equations were integrated for 1.5 ns with a time step of 0.25 fs. The temperature of the system was controlled using Berendsen thermostat. The bond order cut-off of 0.3 was used to identify the size of the water cluster and to identify the instantaneous position of protons.

Results and Discussion

Diffusion of Water Inside Zeolite Channels

Fig. 4 shows the dependence of the water diffusion coefficient on temperature while Table 1 compares the calculated diffusion coefficient with experimental results for the silicalite. It can be seen that the ReaxFF diffusion coefficient is in excellent agreement with PFG NMR experiments[40]. In the simulated temperature range (300K-500K), it can be seen that the diffusion coefficient increases with temperature and this temperature dependence is linear for silicalite and non-linear for H-ZSM-5 zeolite. With an increase in temperature, the number of hydrogen bonds per water molecule decreases and the interaction between water molecules and the framework diminishes. As a result, the water molecules can move faster through zeolite channels. In addition to this temperature dependence, the results also show that water diffuses slowly in the acidic framework than in silicalite. This reduced diffusivity is mainly due to enhanced adsorption of water molecules near acidic centers of H-ZSM-5 zeolite.

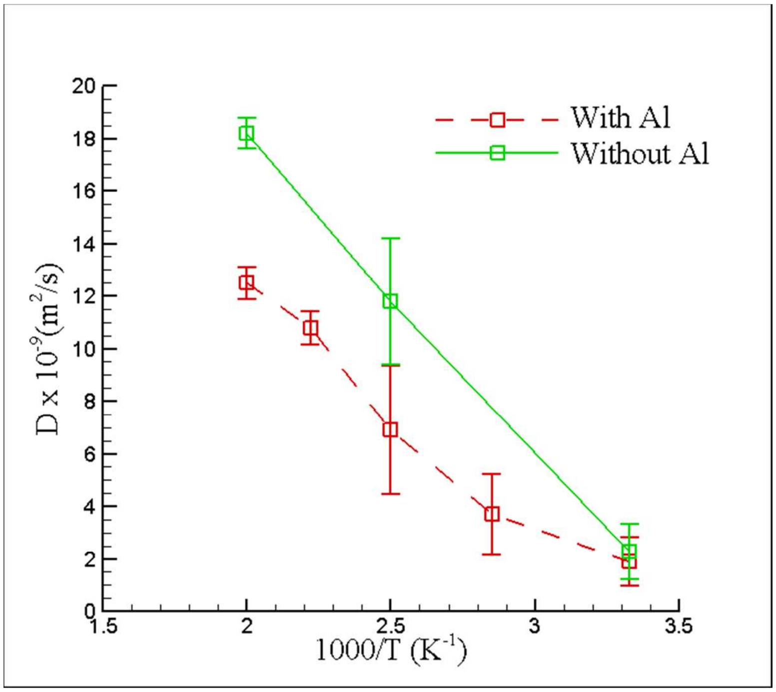

Fig. 4 Diffusion coefficient of water in silicalite and H-ZSM-5 zeolite. Error bars represent standard deviation

Table 1. Comparison of simulated diffusion coefficient with experimental measurements

	ReaxFF	Experimental[40]
Diffusion coefficient (300K) (m^2/s)	1.91×10^{-9}	$1.0 – 4.0 \times 10^{-9}$

Acidity of H-ZSM-5 zeolite

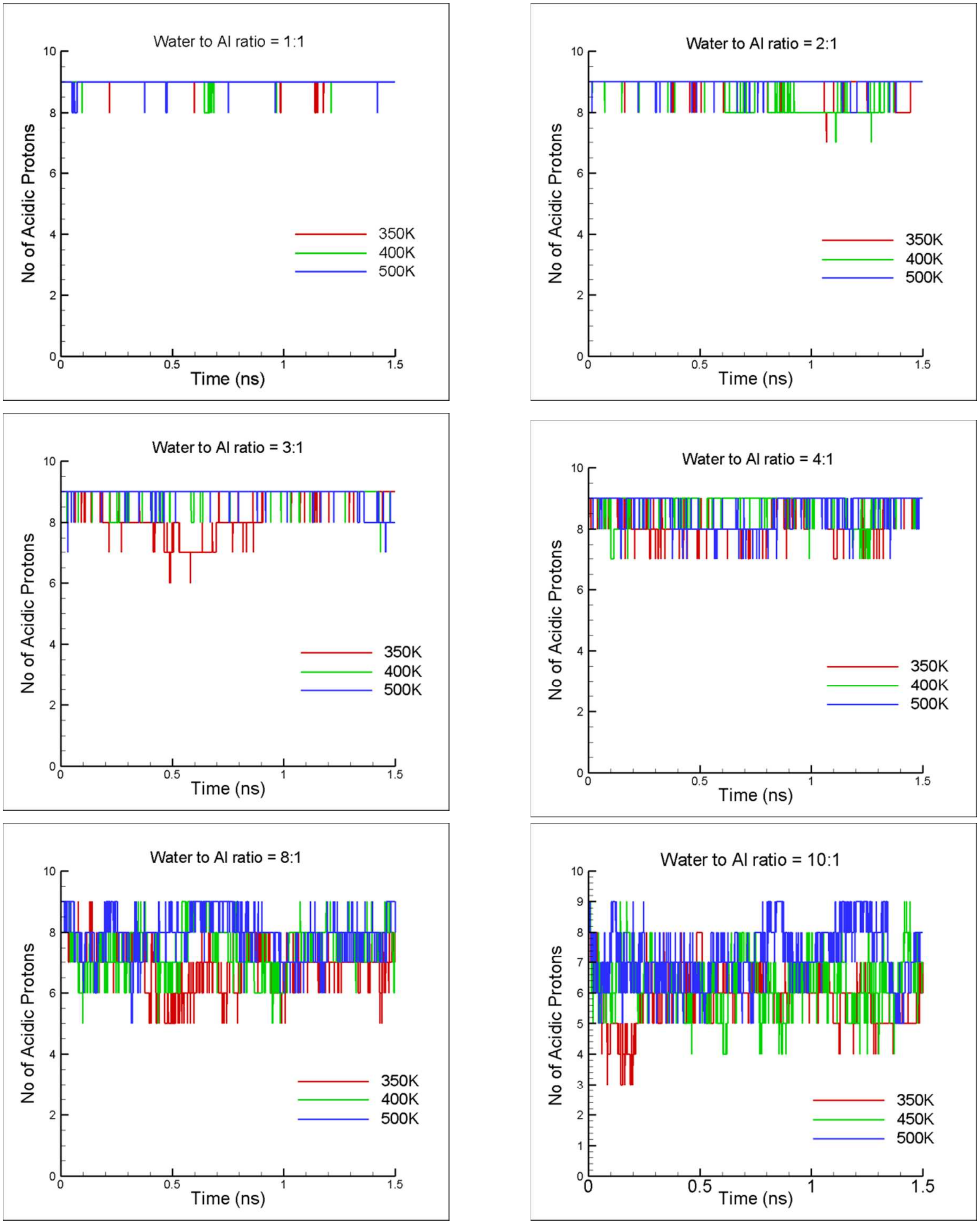

Fig. 5 Effect of water loading and temperature on acidity of zeolite

Fig. 5 shows how the temperature and water loading influence the position of proton inside H-ZSM-5 zeolite channels. In the above figure, acidic proton is defined as hydrogen atom that is chemically attached to framework oxygen atom adjacent to Al center. It can be seen that at low water loadings (water to Al ratio of 1:1 and 2:1), the zeolite retains most of its acidic protons at all temperatures. The discontinuous peaks show few instances in which acidic protons migrated from zeolite to water molecules forming hydronium ions. However, such ions are unstable at low water concentrations and the protons quickly fall back to the zeolite catalyst. With further addition of water inside the zeolite channels, the zeolite framework starts losing its acidity to the water phase. This depletion of acidity increases progressively with the increase in water concentration. The acidity of the zeolite framework also depends upon the temperature. The MD results show that for a given water concentration, the zeolite framework has higher acidity at higher temperature than at lower temperatures. This is mainly because protonated water clusters are more stable at lower temperatures than higher temperatures. As a result, although reactive events corresponding to proton transfer from zeolite to water molecules are frequent at higher temperatures, the resulting protonated water clusters have a shorter life at elevated temperature and consequently, the acidic protons fall back to the zeolite catalysts.

Reaction Pathways

Using the trajectories obtained from MD simulations, we evaluated various reaction pathways. For this reaction analysis, we used bond order cut-off of 0.3 for identifying the molecules. The reactions that were observed in the MD simulation can be broadly divided into two categories, proton transfer from zeolite to water phase and cluster growth and proton hopping between water molecules.

1. Proton transfer from zeolite to water molecules:

For all water loadings, the most dominant reaction pathway involves proton transfer from zeolite to single water molecule forming a hydronium ion (Eq.3). The backward reaction is as frequent as the forward reaction and as a result the protons moves back and forth several times before forming a stable hydronium ion.

$$Z\text{-}H + H_2O \leftrightarrow Z^- + H_3O^+ \qquad (3)$$

At low water loadings (1:1 and 2:1 ratio), we found that proton transfer occurs exclusively by equation 3. In 1.5ns simulation, for 1:1 ratio, we found 67 instances of forward reaction and 67 events of backward reaction. This shows that the hydronium ion is unstable as it is less likely to grow into water clusters and as a result, the protons eventually return to zeolite catalyst. This observed trend at lower water loading agrees well with existing experimental[41] and ab-initio calculations[14].

Table 2. Number proton transfer attempts (Eq. 3) as a function of water loading and temperature

Water to Al ratio	350K	400K	500K
1:1	67	67	46
2:1	200	174	130
3:1	349	299	239
4:1	521	473	376
8:1	824	863	851
10:1	897	1013	861

Table 2 shows the number of proton transfer attempts made at 350K for various loadings. It can be seen that the number of attempts increases progressively with water concentration. Although the reverse reaction is equally likely at all conditions, at higher water loadings, the resulting hydronium ions have a higher chance of forming water clusters such as $H_5O_2^+$ and $H_7O_3^+$. As a result, after several unsuccessful attempts, few hydronium ions can survive by solvating themselves with surrounding water molecules and such formation of stable clusters favors the deprotonation of the framework as protons are retained by the water phase. In systems with higher water content, we also found following two additional reaction pathways involving proton transfer from the zeolite to the water phase.

$$\text{Z-H--}H_2O + H_2O \leftrightarrow Z^- + H_3O^+ + H_2O \qquad (4)$$

$$\text{Z-H} + H_2O + H_2O \leftrightarrow Z^- + (H_3O^+\text{--}H_2O) \qquad (5)$$

Both of these pathways involve two water molecules and we found that the frequency of reactions 4 and 5 increases progressively with amount of water present in the zeolite. The calculations indicate that although the frequency of reaction 5 is far less than reaction 3, the resulting $H_5O_2^+$ cluster has a higher survival probability than isolated hydronium ion formed in reaction 3. It is worthwhile to note that the recent[5] FTIR adsorption study of H_2O in the isostructural H-SSZ-13 and H-SAPO-34 also demonstrated that H_3O+ is not formed in appreciable amount upon H_2O adsorption but at high coverages, H_2O generates clusters that have a proton affinity sufficiently high to abstract protons from the zeolite framework. This suggests that the stability of protonated clusters is more of a function of temperature and water loading compared to framework acidity.

2. Cluster growth and proton hopping reactions

Once the zeolite framework donates a proton to the water phase, then the resulting hydronium ions/clusters can react with other water molecules through different reaction channels. At low water loadings, the hydronium ions were short lived and hence we observed very few events of cluster formation and proton hopping. On the contrary, for medium and high water loadings, cluster formation and proton hopping reactions were frequent during 1.5 ns simulation time. Similar to deprotonation reactions, for most of these proton hopping reaction pathways, backward reactions are equally likey as the forward reaction and this shows that the chemical composition of the system changes very fast giving rise to short lived molecular species.

Table 3. Number of instances of different cluster growth reactions at 350K.

Reaction pathway	4:1	8:1	10:1
$H_3O^+ + H_2O \rightarrow H_5O_2^+$	876	2653	3753
$H_3O^+ + H_2O + H_2O \rightarrow H_7O_3^+$	28	165	264
$H_5O_2^+ + H_2O \rightarrow H_7O_3^+$	8	115	298

Table 3 shows the most frequently observed chemical pathways involved in a growth of water clusters. It can be seen that the tendency to form bigger clusters increases with an increase in water concentration inside the zeolite. The existence of such stable clusters containing multiple water molecules plays a key role in reducing the acidity of zeolite catalysts at higher water concentrations. In simulation with 10:1 hydration ratio, we also found few chemical events leading to formation of $H_9O_4^+$ clusters. This trend indicates that with more water, one can form even bigger water clusters inside the zeolite pores. The average life of such water clusters depend significantly on temperature. At higher temperatures, the stability of such clusters decreases and as a result, less number of chemical events corresponding to cluster growth is found at 500K.

Besides the cluster growth, water molecules/clusters carrying acidic protons also contribute significantly to intermolecular proton hopping and water exchange reactions. Reactions 6-8 list the most dominant of such pathways that were observed in MD simulations.

$$H_5O_2^+ + H_2O \leftrightarrow H_2O + H_5O_2^+ \tag{6}$$
$$H_3O^+ + H_2O \leftrightarrow H_2O + H_3O^+ \tag{7}$$
$$H_7O_3^+ + H_2O \leftrightarrow H_2O + H_7O_3^+ \tag{8}$$

Reactions 6-8 were observed several times in MD simulations. Such constant interchange of protons and water molecules among water clusters indicate that these intermediate cluster/ions have very short life and play a key role in moving protons inside zeolite channels. It also suggests that one requires some tracers to trace the hopping trajectory of acidic protons and characterization methods based on immediate neighbor interaction will not capture the short lifetime of protonated clusters.

Position of protons inside zeolite channels

Fig. 6 shows the probability distribution of the position of the proton carrying oxygen atoms in aqueous phase from the nearest Al neighbor. For this analysis, distance of 10Å is partitioned into 100 bins each separated by 0.1Å. Then, distance between each proton carrying oxygen and Al center of zeolite is calculated. For each proton carrying oxygen atom, only the distance to the nearest Al atom was counted towards obtaining the distribution. This analysis provides very useful information about average position of acidic proton from Al dopants. It can be seen the

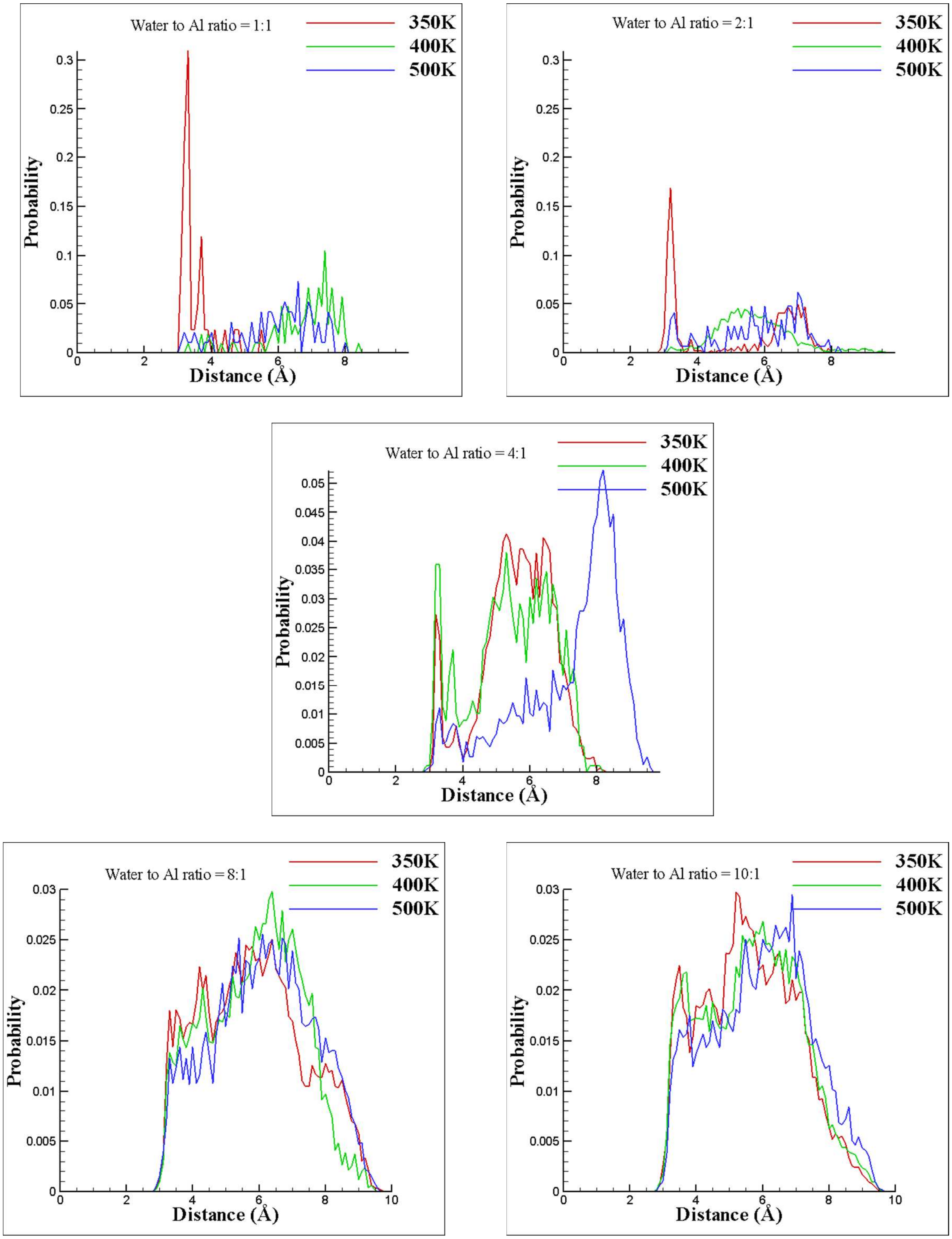

Fig. 6 Position of proton from Al centers of zeolite framework

Al-proton distance distribution depends both on temperature and water loading. It should be noted that for low water loadings (1:1 and 2:1 ratios), less hydronium ions are formed and as a result, the obtained probability distribution is based on small sample size. For 1:1 ratio, at 350K, the acidic protons are most likely to remain within 4Å from Al atoms indicating the existence of short lived adsorption complex. However, with the increase in temperature, the short distance peak diminishes resulting into a broader probability distribution. This broader distribution at 500K is due to two main reasons. At higher temperatures, the hydronium ions can overcome adsorption barrier and can diffuse through the zeolite channels. The second reason for broader distribution is proton hopping among the water molecules. Similar trends are observed for the case of two water molecules per Al atom. The intensity of the short-distance peak is considerably lower for 2:1 water loading indicating the increased influence of diffusion and proton hopping reactions.

The probability distribution for medium loading (4:1 ratio) is a mix of low and high water loading conditions. At 350K and 400K, we can see two distinct peaks. The first peak corresponds to the adsorption complexes between hydronium ions and the zeolite framework. The distribution function also contains a second peak of equal intensity and this additional peak indicates that at medium loading, protons are able to move inside the zeolite channels by diffusion and by hopping. For higher water loading (8:1 and 10:1), the protons are more likely to be 6-8 Å away from Al atoms. This shift in the dominant peak indicates that in the presence of more water molecules, protons can move away from Al centers by hopping between water molecules. At higher water loading conditions, the system is more likely to form water clusters such as $H_5O_2^+$, $H_7O_3^+$ and $H_9O_4^+$. The presence of such clusters provides easier avenues for proton hopping thereby increasing the mobility of protons within the channels. Once the proton moves away from Al atoms, then it cannot fall back to the framework immediately and this factor contributes significantly in reducing the overall acidic strength of the zeolite framework.

Conclusions

We have refitted ReaxFF parameters to improve the description of the interaction between water molecules and zeolite solid catalyst. The optimized parameters are able to reproduce energetics of adsorption of water molecules inside H-ZSM-5 zeolite and of reaction pathway of protonation of water molecules inside the zeolite. The ReaxFF diffusion coefficient of water molecules inside silicalite is in excellent agreement with PFG NMR experimental measurements. The RMD simulations show that the position of acidic protons inside H-ZSM-5 framework depends upon both the water loadings and temperature. At lower water loadings, proton transfer from zeolite to water molecule is not favored and as result, the zeolite retains all the acidic protons. In agreement with experiments[5], H_3O^+ is not stable at low water loadings. However, the probability of proton transfer to the aqueous phase increases progressively with increase in water concentration as hydronium ions can stabilize themselves by forming clusters with other water molecules. Temperature plays an important role on acidity by impacting the mobility of water molecules to diffuse in addition to adsorption and it also decreases the number of hydrogen bonded interactions between the framework and water clusters and within water clusters. At higher temperatures, such protonated clusters become less stable and as a result acidic protons move back to the zeolite framework. This loading and temperature dependence observed in RMD calculations is in good agreement with existing experimental results.

We found two dominant reaction channels in RMD simulations, namely, proton transfer from zeolite framework to water molecules and subsequent cluster growth; and proton hopping between water molecules and water clusters. The tendency to form bigger clusters increases with increase in water concentration. Such bigger clusters provide easier avenues for proton hopping and as a result, protons have higher probability of moving away from Al centers of the zeolite at higher water loadings. This enhanced mobility of protons plays a key role in depleting acidic strength of H-ZSM-5 zeolite at lower temperatures. Efforts are underway to study the competition of acidity to the protonation ability of methanol and water mixtures and to understand acidity dependence as a function of Al distribution in H-ZSM5.

Acknowledgement

ACTvD acknowledges funding from the U.S. Department of Energy, Office of Basic Energy Sciences, Division of Chemical Sciences, Geosciences and Biosciences.

References

1. A. Corma, *Chem. Rev.*, 1997, **97**, 2373.

2. C. Baerlocher, L. B. McCusker, and D. Olson, *Atlas of Zeolite Framework Types*, Elsevier B.V., Amsterdam, Sixth., 2007, 212-213

3. D. H. Olson, W. O. Haag, and R. M. Lago, *J. Catal.*, 1980, **61**, 390.

4. F. Wakabayashi, J. N. Kondo, K. Domen, and C. Hirose, *J. Phys. Chem.*, 1996, **100**, 1442–1444.

5. S. Bordiga, L. Regli, C. Lamberti, A. Zecchina, M. Bjørgen, and K. P. Lillerud, *J. Phys. Chem. B*, 2005, **109**, 7724–32.

6. P. Sazama, Z. Tvaruzkova, H. Jirglova, and Z. Sobalik, in *Proceedings of 4th International FEZA Conference*, 2008, vol. 5, pp. 821–824.

7. L. Smith, A. K. Cheetham, R. E. Morris, L. Marchese, J. M. Thomas, P. A. Wright, and J. Chen, *Science (80-.).*, 1996, **271**, 799–802.

8. A. Alberti and A. Martucci, *J. Phys. Chem. C*, 2010, **114**, 7767–7773.

9. M. Krossner and J. Sauer, *J. Phys. Chem.*, 1996, **100**, 6199–6211.

10. S. A. Zygmunt, *J. Phys. Chem. B*, 2001, **105**, 3034–3038.

11. C. Tuma and J. Sauer, *Chem. Phys. Lett.*, 2004, **387**, 388–394.

12. J. Limtrakul, P. Chuichay, and S. Nokbin, *J. Mol. Struct.*, 2001, **560**, 169–177.

13. Y. Jeanvoine, G. Angyan, Janos, G. Kresse, and J. Hafner, *J. Phys. Chem. B*, 1998, **102**, 7307–7310.

14. M. V Vener, X. Rozanska, and J. Sauer, *Phys. Chem. Chem. Phys.*, 2009, **11**, 1702–1712.

15. M. Fleys, R. W. Thompson, and J. C. Macdonald, *J. Phys. Chem. B*, 2004, **108**, 12197–12203.

16. J. Z. Yang, Q. L. Liu, and H. T. Wang, *J. Memb. Sci.*, 2007, **291**, 1–9.

17. F.-X. Coudert, F. Cailliez, R. Vuilleumier, A. H. Fuchs, and A. Boutin, *Faraday Discuss.*, 2009, **141**, 377–398.

18. J. Kuhn, J. M. Castillo-sanchez, J. Gascon, S. Calero, D. Dubbeldam, T. J. H. Vlugt, F. Kapteijn, and J. Gross, *J. Phys. Chem. C*, 2009, **113**, 14290–14301.

19. C. E. Ramachandran, S. Chempath, L. J. Broadbelt, and R. Q. Snurr, *Microporous Mesoporous Mater.*, 2006, **90**, 293–298.

20. A. Ö. Yazaydın and R. W. Thompson, *Microporous Mesoporous Mater.*, 2009, **123**, 169–176.

21. M. V. Vener and N. B. Librovich, *Int. Rev. Phys. Chem.*, 2009, **28**, 407–434.

22. E. S. Stoyanov, I. V. Stoyanova, and C. a. Reed, *Chem. Sci.*, 2011, **2**, 462.

23. J. M. J. Swanson and J. Simons, *J. Phys. Chem. B*, 2009, **113**, 5149–61.

24. C. Knight and G. a Voth, *Acc. Chem. Res.*, 2012, **45**, 101–9.

25. S. Lammers, S. Lutz, and M. Meuwly, *J. Comput. Chem.*, 2008, **29**, 1048–1063.

26. M. G. Wolf and G. Groenhof, *J. Comput. Chem.*, 2014, **35**, 657–71.

27. A. C. T. van Duin, S. Dasgupta, F. Lorant, and W. A. Goddard, *J. Phys. Chem. A*, 2001, **105**, 9396–9409.

28. K. Chenworth, A. C. T. van Duin, and W. A. Goddard, *J. Phys. Chem. A*, 2008, **112**, 1040.

29. E. G. Goken, K. L. Joshi, M. F. Russo, A. C. T. van Duin, and A. W. Castleman, *J. Phys. Chem. A*, 2011, **115**, 4657–64.

30. J. G. O. Ojwang, R. van Santen A., G. J. Kramer, A. C. T. van Duin, and W. A. Goddard III, *J. Chem. Phys.*, 2008, **129**, 244506.

31. M. R. LaBrosse, J. K. Johnson, and A. C. T. van Duin, *J. Phys. Chem. A*, 2010, **114**, 5855.

32. K. Chenworth, A. C. T. van Duin, P. Persson, M. J. Cheng, J. Oxgaard, and W. A. Goddard, *J. Phys. Chem. C*, 2008, **112**, 14645.

33. M. Aryanpour, A. C. T. van Duin, and J. D. Kubicki, *J. Phys. Chem. A*, 2010, **114**, 6298.

34. K. L. Joshi and A. C. T. Van Duin, *Energy Fuels*, 2013, **27**, 4481.

35. J. A. Ryder, A. K. Chakraborty, and A. T. Bell, *J. Phys. Chem. B*, 2000, **104**, 6998–7011.

36. A. D. Bochevarov, E. Harder, T. F. Hughes, J. R. Greenwood, D. A. Braden, D. M. Philipp, D. Rinaldo, M. D. Halls, J. Zhang, and R. A. Friesner, *Int. J. Quantum Chem.*, 2013, **113**, 2110–2142.

37. C. Chiu, G. N. Vayssilov, A. Genest, A. Borgna, and N. Rosch, *J. Comput. Chem.*, 2014, **35**, 809.

38. H. J. C. Berendsen, J. P. M. Postma, W. F. Van Gunsteren, A. Dinola, and J. R. Haak, *J. Chem. Phys.*, 1984, **81**, 3684.

39. M. P. Allen and D. J. Tildesley, *Computer Simulation of Liquids*, Oxford University Press, New York, NY, 1991, 182-211

40. C. Bussai, S. Vasenkov, H. Liu, W. Böhlmann, S. Fritzsche, S. Hannongbua, R. Haberlandt, and J. Kärger, *Appl. Catal. A*, 2002, **232**, 59–66.

TOC Figure

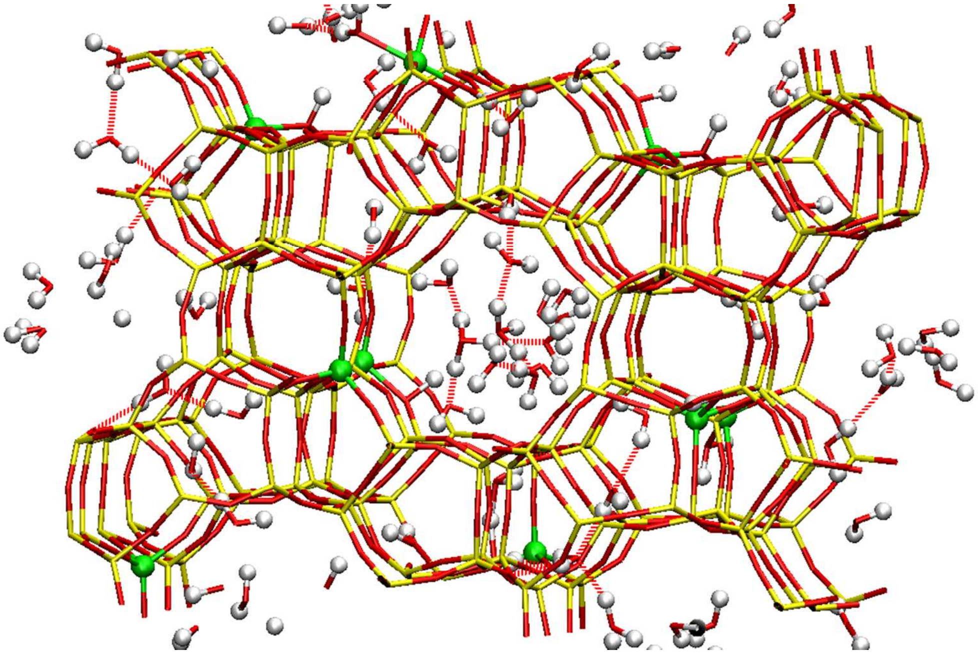

Protonation of water inside H-ZSM-5 zeolite using the ReaxFF reactive force field method.